Environmental Science Advances

ROYAL SOCIETY OF CHEMISTRY

PAPER

View Article Online
View Journal | View Issue

Cite this: *Environ. Sci.: Adv.*, 2024, **3**, 950

Organic matter concentration and characteristic dynamics in surface waters post-bushfires and cyclones: fDOM sensors for environmental monitoring and control†

Hiua Daraei, *[abc] Edoardo Bertone, [bcd] Rodney A. Stewart,[bc] John Awad,[ae] Adam Leavesley,[f] Matthew Gale,[g] Eriita Jones,[ah] Kathy Cinque,[i] Mark Agnew,[j] Hugh A. Burger[a] and John Van Leeuwen [a]

This study presents the findings of an investigation on the dynamics of dissolved organic matter (DOM) concentration and characteristics of four Australian rivers and reservoirs after their catchments had been severely burned by bushfires (wildfires) or impacted by a tropical cyclone. Dissolved organic carbon (DOC) increased immediately following the events, and subsequently decreased. The findings indicate rapid stabilisation of water quality, based on the measured parameters, following the commencement of the first winter after the events (which occurred in mid/end summer). In the fire-affected Middle River catchment, DOC decreased from 30.7 mg L^{-1} to 10.2 mg L^{-1} over approximately seven months. In the case of the Herring Lagoon catchment, which was affected by cyclone Uesi, DOC decreased from 15.6 mg L^{-1} to 1.2 mg L^{-1} over approximately ten months. However, the DOM present in the surface water exposed to the cyclone showed higher molecular weight, coagulability and UV-vis absorbance than the DOM present in the surface water of fire-affected catchments. The observed rapid increase and then reduction in DOM concentrations after extreme climate events indicates the need for short-term and rapid responses for drinking water treatment. The fluorescence signal of a field-deployable fluorescent DOM (fDOM) sensor showed potential as an online monitoring tool for assessing DOM concentration in surface waters, including under extreme conditions. The rapid identification of high DOM loadings in surface waters following extreme climate events (*e.g.* using a field deployed fDOM sensor) along with its coagulability characteristics could assist in catchment management and drinking water treatment by enabling timely control decisions in response to the impacts of such events.

Received 5th February 2024
Accepted 1st May 2024

DOI: 10.1039/d4va00036f

rsc.li/esadvances

Environmental significance

Understanding the impact of natural disasters on water sources is vital for resilience and resource management. This study reveals the response of dissolved organic matter (DOM) concentration and characterisation in surface water sources to severe bushfires and a tropical cyclone. Post-event, DOM concentrations initially surged, followed by a rapid decline, indicating water quality stabilisation within the first winter. Despite similar concentration trends, DOM characteristics differed between fire-affected and cyclone-impacted waters, suggesting varied impacts on treatment processes and ecological health. The research emphasises the need for swift drinking water treatment responses to extreme climate events. The deployment of a field fluorometer proves promising for real-time DOM monitoring, aiding catchment management and enabling timely decision-making for water treatment in the aftermath of environmental crises.

[a]*Sustainable Infrastructure and Resource Management (SIRM), UniSA STEM, University of South Australia, Mawson Lakes, South Australia, 5095, Australia*

[b]*Griffith School of Engineering and Built Environment, Griffith University, Parklands Drive – Gold Coast Campus, Southport, Queensland, 4222, Australia. E-mail: H. Daraei@Griffith.edu.au; Tel: +61-7-555-28574*

[c]*Cities Research Institute, Griffith University, Parklands Drive, Southport, Queensland, 4222, Australia*

[d]*Australian Rivers Institute, Griffith University, 170 Kessels Road, Nathan, Queensland, 4111, Australia*

[e]*CSIRO Environment, Waite Campus, Waite Rd., Urrbrae, South Australia, 5064, Australia*

[f]*Parks and Conservation Service, Environment, Planning and Sustainable Development Directorate, Australian Capital Territory (ACT), 2601, Australia*

[g]*Fenner School of Environment & Society, Australian National University, ACT, 2601, Australia*

[h]*School of Earth and Planetary Sciences, Curtin University, Perth, WA 6845, Australia*

[i]*Melbourne Water, LaTrobe Street, Docklands, Victoria 3008, Australia*

[j]*Kangaroo Island Landscape Board, 35 Dauncey St, Kingscote, South Australia, 5223, Australia*

† Electronic supplementary information (ESI) available. See DOI: https://doi.org/10.1039/d4va00036f

1 Introduction

Extreme climate events can cause the quality of surface drinking water sources to deteriorate through the degradation of catchments, water flow pathways, and storage reservoirs. These events can impact drinking water treatment processes and infrastructure, and the quality of distributed water.[1,2] Heavy rainfall and floods (including those associated with cyclones) can significantly increase turbidity and dissolved organic carbon (DOC) loads in surface waters from terrestrial (allochthonous) sources.[3] This can change dissolved organic matter (DOM) pool characteristics and treatability, impacting the disinfection by-product formation potential in treated water.[4]

Bushfires are a feature of the Australian landscape, that occur following extended periods of dry weather conditions.[5,6] Extreme events such as the 2019–2020 Australian bushfires have been attributed to the effects of anthropogenic climate change, which has driven increased temperature extremes and long-term warming.[6,7] Large-scale bushfires can be detrimental to surface water catchments and associated water stream quality, which is an ongoing concern. This can occur through an increase in catchment runoff following such events, which can transport sediments, ash, soluble organic materials, heavy metals and nutrients into waterways.[8–10] Bushfires can therefore elevate risk of algal/cyanobacterial blooms in surface waters due to elevated nutrient inflows.[4,11] Extremely high levels of turbidity (up to 4200 NTU), appearing as pitch-black water, were reported for the Murray River after the 2019–2020 Australian bushfires.[9] Bushfires can lead to elevated concentrations of organic compounds, including dioxins and fire pyrolysis products such as polycyclic aromatic hydrocarbons, polychlorinated dibenzo-ρ-dioxins and dibenzofurans and polychlorinated biphenyls, which could pose challenges for conventional water treatment processes.[12–16] Exposure of these organic compounds to chlorine during the disinfection process may lead to the formation of halogenated disinfection by-products, which can pose health concerns[12–14] or provide a substrate for microbial regrowth in drinking water distribution systems.[17]

High DOM concentrations can have a significant impact on freshwater ecosystems. Dissolved organic matter is a substrate for microbial growth that fuels microbial-based food webs[18,19] and transport metal ions including heavy metals.[20] Moreover, high DOM concentrations can attenuate light penetration, which consequently limits photosynthetic activity in the water body.[21] Conversely, DOM induced attenuation of the ionising irradiation portion of light (*e.g.* ultraviolet light) can protect aquatic organisms from its hazardous impacts.[21] High DOM concentrations can occur due to transport of terrestrial organic matter when catchments become inundated with surface water flows following heavy rainfall.[22] This can elevate heterotrophic bacterial activity, deplete oxygen, and kill aquatic organisms.[23] Nonetheless, extreme events such as bushfires and cyclones can also be beneficial by supplying food and nutrients, which increases river productivity and benefits waterbirds, native fish and other aquatic organisms.[23]

Few studies have examined the concentration and characteristics of DOM in waterways after fires. Johnston and Maher (2022)[24] studied flow-stratified water quality data from a large coastal catchment (Macleay River, Australia) spanning severe drought and extensive fires followed by flooding. They reported that the levels of several water constituents including suspended sediment, PO_4, NO_3, DOC, K, Ca, SO_4, HCO_3, Mg, Cl, Na, and NH_4 were highly elevated (*i.e.* >100, 22, 21, 7.8, 7.4, 5.7, 4.7, 3.9, 3.6, 2.1, 1.6 and >104 times, respectively) during the initial post-fire period (comparison of the maximum post-fire concentrations with pre-fire median concentrations). The observed ion concentration order was reported to reflect the composition of the ash materials. They reported a fast biogeochemical cycling of dissolved inorganic nitrogen species during initial flow events following the fire, with NH_4–N initially dominant (>80% of dissolved inorganic nitrogen [DIN]) and exceeding ecosystem guideline threshold values (>100 μM NH_4–N), followed by rapid (approximately one week) nitrification. Sherson *et al.* (2015)[25] and Johnston and Maher (2022)[24] emphasised the necessity for high-frequency sampling to adequately capture the impacts of drought, fires, and floods on aquatic systems due to the high temporal variability of water quality parameters. Another study by Basso *et al.* (2021)[26] on boreal sub-arctic lake water chemistry throughout a summer in northern Alberta, where almost 30% of the area that flows into the reservoir was affected by a bushfire, showed substantial increases in dissolved nitrogen (1.2 times), dissolved phosphorus (2 times) and DOC (1.5 times) compared to reference lakes. These increases were accompanied by a 9% reduction in mean pH. Similarly, Sherson *et al.* (2015)[25] studied nutrient dynamics in a stream following a bushfire (the Las Conchas bushfire in June 2011 that burned approximately 36% of the contributing watershed) and during several precipitation events using water quality sensors. They found significant increases in dissolved NO_3–N (6 times the background levels), dissolved phosphate (100 times the background levels), specific conductance (5 times the background levels) and turbidity (>100 times the background levels). These increases were noted to be accompanied by reductions in dissolved oxygen and pH, as reported by Sherson *et al.* (2015)[25]. The study highlighted the rapid rates of change in water quality during flow events of short duration following bushfires. White *et al.* (2006)[27] reported increases (up to thirty times) in turbidity, iron and manganese in the upper catchment storages following a bushfire. These were problematic to water supply, resulting in the construction of a drinking water treatment plant (DWTP) for turbidity removal. White *et al.* (2006) also reported the impact of natural revegetation in the catchment on the improvements in water quality.

The environmental risks associated with extreme climate events demonstrate the need for high-frequency water quality monitoring of vulnerable drinking water sources.[4,28] Online, real-time monitoring systems may assist in providing treatment and disinfection for impacted influent surface water in water treatment plants (WTPs).[29] Hurst *et al.* (2004)[29] proposed the integration of an online DOC analyser with a model-based coagulation control system to determine the required coagulant

dose for waters varying in DOC variation circumstances during extreme events. Moreover, fluorescent DOM (fDOM) sensors can detect fluorescence signals from the fluorophore portion of the DOM pool. The fDOM sensor signal can be used as either semi-quantitative (as a surrogate parameter to estimate DOC concentration) or semi-qualitative (DOM pool optical and coagulability characteristics) information.[30,31] Field fDOM measurements are prone to interference from signal attenuation/quenching factors, such as temperature, turbidity, pH, and the inner filter. Interference with the fDOM signal can be exacerbated in water sources impacted by extreme climate events, though this aspect requires further investigation.

The impacts of bushfires and cyclones on water quality have been widely investigated. However, investigations have focused predominantly on the discharge of sediments, ash, turbidity, dissolved metals, DOM concentration, and nutrients (N and P) discharged from catchments into waterways.[2,9,10,25,32,33] This study used multi-analytical techniques to investigate DOM concentration and characteristics, Chlorophyll-a (Chla) and turbidity following bushfires and a cyclone. This is reported for (1) river waters of two Australian catchments following the extreme bushfire events in the summer of 2019/2020 over a period of approximately two years, and (2) two reservoirs impacted by Tropical Cyclone Uesi in 2020 over a period of approximately one year. We also investigated the application of the EXO fDOM sensor signal for monitoring DOM concentration and characteristics, in comparison with the DOC and A_{254} indices.

2 Materials and methods

2.1 Study area

Water samples ($n = 51$) were collected between September 2019 and November 2021 from four water sources in Australia: 25 from the Orroral River (P01) site located in the Australian Capital Territory (ACT), 6 from the Leslie Harrison Dam (P03) and Herring Lagoon (P05) sites located in Queensland (QLD) and 20 from the Middle River (P11) site located in South Australia (SA) – see Fig. 1 and Table A1, ESI.† The water sampling points were coded, as detailed above and as previously reported.[34,35] Of the catchments investigated, only the Orroral River (P01) is not used for drinking water supplies.

The P03 and P05 sites experienced Tropical Cyclone Uesi on February 4–14, 2020, QLD[36,37] – see Table S1, ESI.† The P01 and P11 sites experienced severe bushfires from December 2019 to February 2020 in Canberra and SA.[38] Liu *et al.* (2022)[39] reported that more than 30% of Kangaroo Island (mainly the western region) burned during a bushfire that occurred between October 2019 and February 2020. Another severe bushfire burned 80% of the Namadgi National Park (Canberra, Australia) area.[40] Cyclone Uesi caused flooding due to storms with up to 220 mm of heavy rain in south-east Queensland.[37,41]

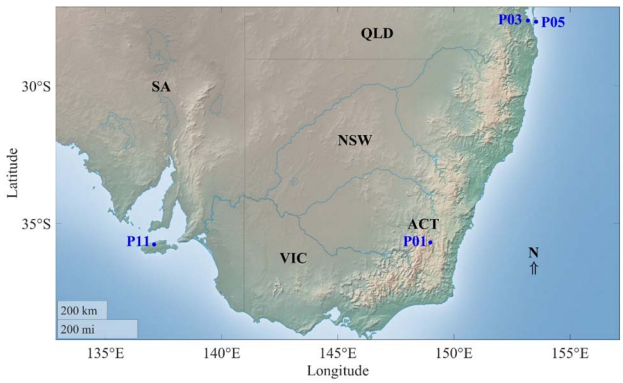

Fig. 1 Water sampling locations – Orroral River (P01), Leslie Harrison Dam (P03), Herring Lagoon (P05) and Middle River (P11).

2.2 Water samples and water quality analyses

Water samples were collected soon after bushfires (coded as P01_01 and P11_01), and for almost two years thereafter (coded as P01_02 to P01_25 and P11_02 to P11_20) – see Fig. 2 and Table S1, ESI.† For the cyclone – a water sample was collected before the event at site P03 (coded as P03_01), two samples were collected soon after the event (coded as P03_02 and P05_01), and three follow up samples were collected for almost one year thereafter (coded as P03_03, P05_02 and P05_03) – see Fig. 2 and Table S1, ESI.†

Multi-analytical techniques – including commonly used and advanced analytical techniques – were used to investigate a wide range of water quality parameters in water samples. Parameters included DOC, A_{254}, colour, EXO $fDOM_s$ (fluorescence excitation/emission [ex/em] wavelengths of [365 ± 5]/[480 ± 40] nm, YSI, Yellow Springs, OH, USA), turbidity, and Chla (using a fluorescence sensor with an ex/em wavelength of [470 ± 15]/[685 ± 20] nm, Xylem Analytics, USA[42]) calibrated using 625 μg per L rhodamine WT dye (66 μg per L Chla), high pressure size exclusion chromatography (HPSEC) with a UVA_{260} detector (HPSEC-UVA_{260}) and HPSEC with a fluorescence-humic detector at an ex/em wavelength of 320/430 (HPSEC-Fl_Hu). The details of the acquisition of some of these water quality parameters (including DOC, A_{254}, colour, EXO $fDOM_s$, and turbidity) have been previously reported.[43] EXO $fDOM_s$ were corrected for turbidity, temperature and pH impacts (referred to as EXO $fDOM_{s,III}$), and EXO $fDOM_{s,III}$ were corrected for the inner filter effect (IFE) impact (referred to as EXO $fDOM_{s,IV}$) following the correction approach presented in Daraei *et al.* (2023).[34] An alkalinity test was conducted for the samples using the titration method.[44]

Specific optical characteristics of DOM were calculated for each sample, namely specific UVA_{254} ($SUVA_{254} = UVA_{254}/DOC$), specific colour (Sp. Colour = Colour/DOC), and specific $fDOM_s$ (Sp. fDOM = $fDOM_s$/DOC). The UV-vis absorbance spectra were collected and analysed as described in Daraei *et al.* (2023).[45]

For a limited number of samples (mostly collected immediately after the events), several additional water quality parameters were acquired. These included total nitrogen (TN), total nitrate plus nitrite, total Kjeldahl nitrogen (TKN), total phosphorus (TP), total organic carbon (TOC), heavy metals, and alkalinity. These data were obtained through a NATA accredited (**https://nata.com.au/**) laboratory (AWQC, SA Water).

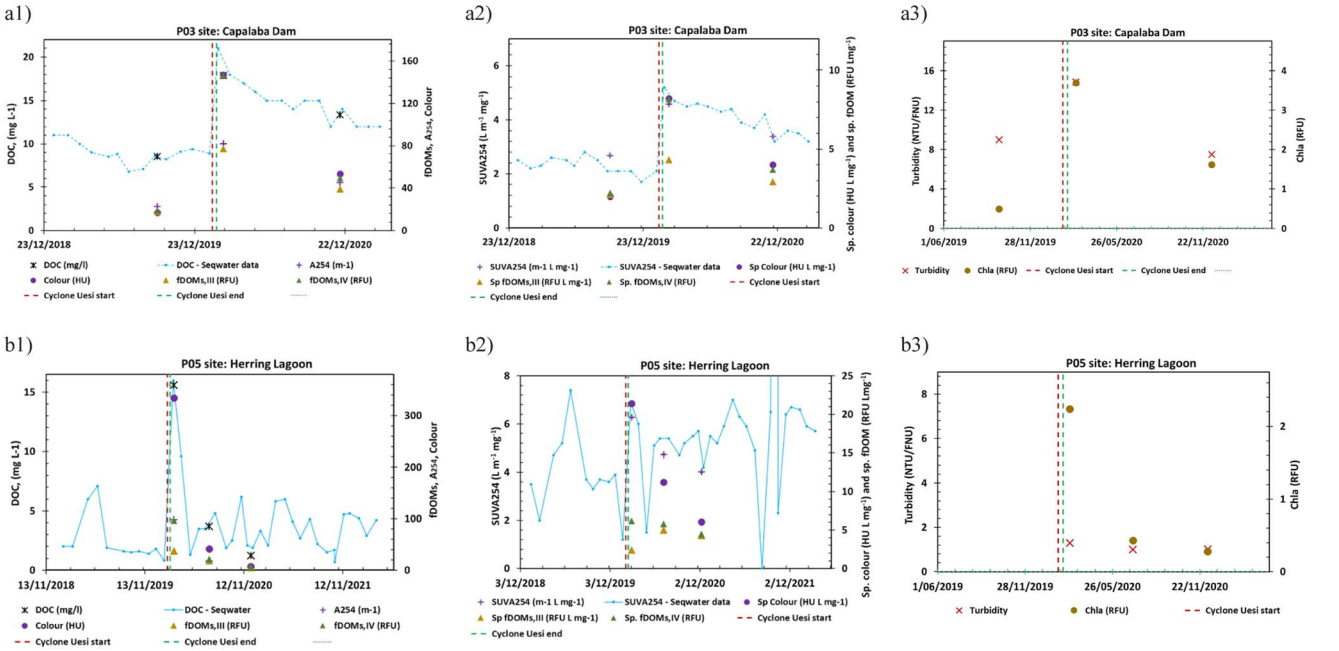

Fig. 2 Chronological variations of (1) DOM concentration (measured as DOC, A_{254}, $fDOM_{s,III}$, $fDOM_{s,IV}$ and colour), (2) DOM optical characteristics (measured as $SUVA_{254}$, Sp. $fDOM_{s,III}$, Sp. $fDOM_{s,IV}$ and Sp. colour) and (3) turbidity and Chla in (a) Leslie Harrison Dam, P03 and (b) Herring Lagoon, P05 surface water sources. *Seqwater (South-East Queensland water authority, Queensland, Australia) recorded DOC and $SUVA_{254}$ data with higher chronological resolution have been added to the diagrams. *Full-page size graphs are provided in the ESI.†

The DOM coagulability, which is defined as the removable DOC percentage by the enhanced coagulation process, and DOM removal rate, which is defined by Daraei *et al.* (2023)[35] as the maximum DOC removal rate per 100 mg alum as $Al_2(SO_4)_3 \cdot 18H_2O$]) during the enhanced coagulation process and in the lower range of applied alum doses (the range with the highest efficiency for removing DOM) were attained using jar test data as previously reported in details in ref. 35 and 45 studies.

2.3 Advanced DOM characteristics and data analysis

Fluorescence excitation-emission matrices (fEEMs, *i.e.* 3D spectra) and HPSEC data (*i.e.* 2D chromatograms) were collected and analysed as described in Daraei *et al.* (2023).[45] These were obtained using an LS55 (PerkinElmer, USA) benchtop fluorometer. fEEMs were corrected before any further data analysis, using a script developed in MATLAB software (according to Murphy *et al.* (2013)[46] instruction). Corrections included blank correction using a Milli-Q water fEEM, masking and smoothing primary and secondary Rayleigh peaks, IFE correction using UV-vis absorbance data, and converting signal intensity to a standardised Raman unit. Following this, fEEMs were analysed through visualisation of the 3D spectra, followed by determination of the biological fluorescence index (BIX, ranging from 0 to 1)[47] and humification fluorescence index (HIX, ranging from 0 to 1),[48] and PARAFAC analysis.[49] Details of the PARAFAC model development for the fEEMs of the water samples, the selection procedure for the number of model components, and the PARAFAC model statistical validation have been previously reported.[43]

HPSEC with UV-detection (HPSEC-UVA_{260}) and humic fluorescence detection (HPSEC-FlHu, $\lambda_{ex/em}$ = 280/330 nm) were performed according to the method of Chow *et al.* (2008)[50] to determine the apparent molecular weight (AMW) profile and weight-average molecular weight (WAMW). The HPSEC data were also analysed using five previously introduced molecular size fractions (area) according to the method described by de Oliveira *et al.* (2018)[31] – see Table A2, ESI† for MW areas and corresponding fractions. The HPSEC data were analysed by a peak fitting technique as previously described in Daraei *et al.* (2023).[45] HPSEC-UVA_{260} chromatograms were partitioned into seven components (peaks, *i.e.* HPSEC-UVA260-PF-P_x peaks) with peak centres corresponding to molecular weights (MWs) of ~457 Da (PF–P_1), 1000 Da (PF–P_2), 1698 Da (PF–P_3), 2454 Da (PF–P_4), 3162 Da (PF–P_5), 4169 Da (PF–P_6) and 36 308 Da (PF–P_7), respectively. The HPSEC-Fl-Hu chromatograms were partitioned into seven components (Peaks, *i.e.* HPSEC-Fl-Hu-PF-P_x peaks) with peak centres (MWs) of ~398 Da (PF–P_1), 776 Da (PF–P_2), 1140 Da (PF–P_3), 1841 Da (PF–P_4), 2690 Da (PF–P_5), 4169 Da (PF–P_6) and 70 280 Da (PF–P_7), respectively. For each sample, the peak centre, peak width and peak height were adjusted using the genetic algorithm (GA) function,[51] and some differences in peak centres are therefore expected among the different samples.

2.4 Precision estimation

Using two water samples, the coefficient of variation (CV) of several key water quality analyses was less than 4.5% for all parameters (except true colour for one sample: CV = 12.1%), as shown in Table A3, ESI.†

3 Results and discussion

3.1 Chronological water quality index variations

The results of DOM concentration and characteristic (commonly used indices) analyses are presented in Fig. $2a_1$ and b_1 (cyclone) and Fig. $3a_1$ and b_1 (bushfires). These data were used for the calculation of $SUVA_{254}$ and specific colour (sp. colour) as common DOM characteristic parameters, as well as sp. $fDOM_s$ parameter (*e.g.* YSI EXO fDOM sensor) and online TOC/DOC analysers. The results of the chronological tracking of turbidity and Chla are also presented in Fig. $2a_3$ and b_3 (cyclone) and Fig. $3a_3$ and b_3 (bushfires).

In most cases, there were similar correlations between DOC and its optical surrogate parameters (*i.e.* A_{254}, colour and corrected $fDOM_s$) as measures for DOM concentration (Table A4, ESI†). This indicates the potential of these optical parameters (signals) for site-specific tracking of DOM concentration, including the sites that experienced the cyclone or bushfires. However, there were different variation rates for these optical parameters (*i.e.* greater changes in colour than A_{254} and fDOM signals; Fig. $2a_1$ and b_1 [cyclone] and Fig. $3a_1$ and b_1 [bushfires]). This might be due to the different DOM fractions and associated optical characteristics. In the case of Fig. $2a_1$, colour changes are approximately two times greater than A_{254}, which may indicate a greater variation in the portion of the humic-like DOM fraction (more associated with the colour index) rather than the protein-like fraction in the total DOM concentration variation. In the case of the EXO fDOM signal, interfering factors such as turbidity and IFE may also cause these different variation rates. Daraei *et al.* (2023)[34] previously reported a study on these interfering factors as well as a correction technique for such interferences.

Seqwater (South-East Queensland water authority, Queensland, Australia) also recorded DOC and $SUVA_{254}$ data which have been added to the data acquired in this study for the P03 and P05 sites (see Fig. 2). This combination of the data, with high temporal resolution and coverage can provide more reliable indicators of bushfire and cyclone effects on the surface water sources than the three-point based datasets we have recorded in our study.

3.1.1 DOM concentration and characteristics (commonly applied indices). High DOM concentrations with high $SUVA_{254}$ occurred immediately after Cyclone Uesi at the P03 and P05 sites. This was followed by a decrease in both DOM concentration and its chromophoric characteristics over time. This may be due to the fresh terrestrial origin of DOM transported to waters by heavy rains from the cyclone.[52] In contrast, a high DOM concentration (up to ~31 mg L^{-1}) but a medium-low level of $SUVA_{254}$ (<4 L m^{-1} mg^{-1}) was observed immediately following the bushfires (P01 and P11 sites). This was followed by a decrease in the DOM concentration and a slight increase in the $SUVA_{254}$ level over time. This could be due to the transport of DOM with a lower chromophoric characteristic from fire (combustion) or subsequent microbial growth conditions. Our post-fire DOM results are similar to those of Sherson *et al.* (2015)[25], who demonstrated an increase in DOM shortly following bushfire events. Chen *et al.* (2020)[53] reported lower coagulability for DOM sourced from the bushfire ash due to the

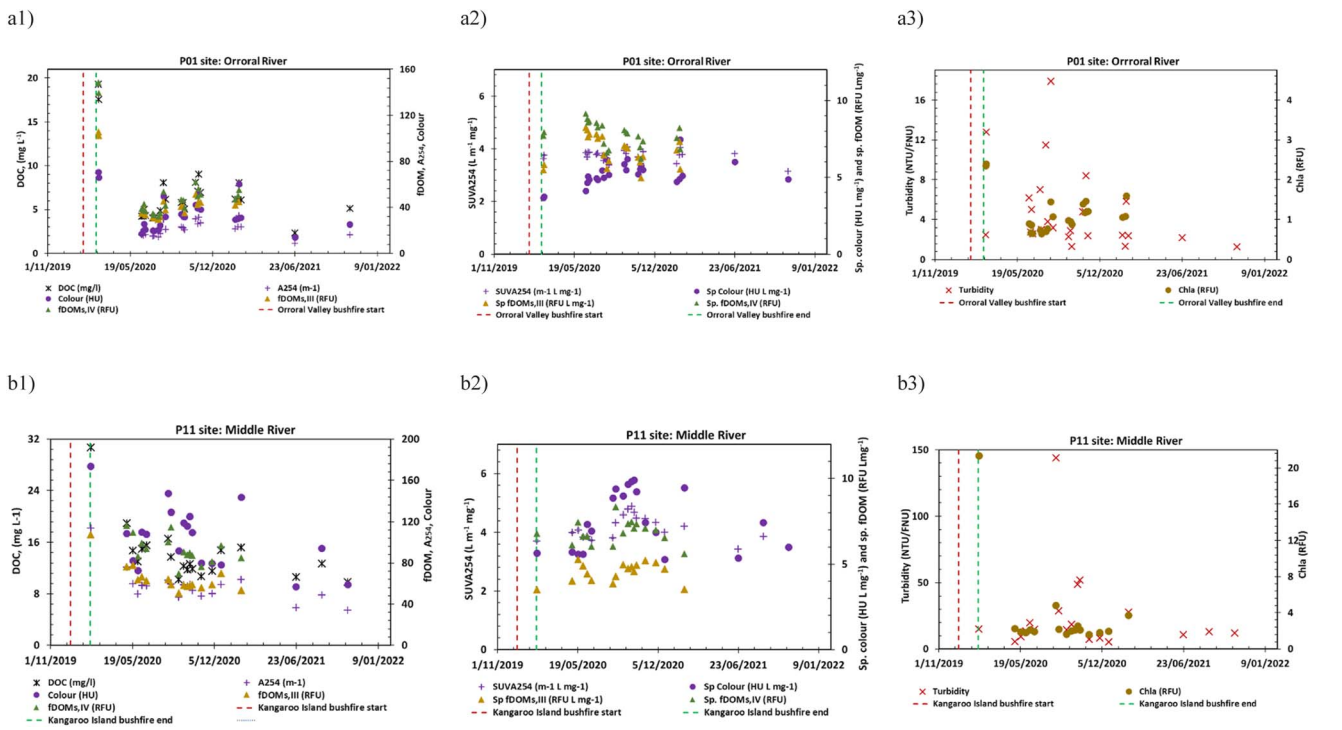

Fig. 3 Chronological variations of (1) DOM concentration (measured as DOC, A_{254}, $fDOM_{s,III}$, $fDOM_{s,IV}$ and colour), (2) DOM optical characteristics (measured as $SUVA_{254}$, Sp. $fDOM_{s,III}$, Sp. $fDOM_{s,IV}$ and Sp. colour) and (3) turbidity and Chla in (a) Orroral River, P01 and (b) Middle River, P11 surface water sources. *Full-page size graphs are provided in the ESI.†

loss of side chains and the decrease in DOM MW. The discharge of such materials can occur *via* (1) airborne ash and smoke, (2) precipitation events and (3) fire extinguishing activities during the bushfire and soon after the event.[52,54,55] Aerosol emissions from bushfires can increase the atmospheric transport of macronutrients and bio-essential trace metals such as nitrogen and iron, respectively.[56] For the Middle River water sample collection site, a layer of ash was present on the surface of the water stream and surrounding soil area.

Xu *et al.* (2024)[57] also observed the emergence of recalcitrant dissolved black carbon (DBC), dissolved black nitrogen (DBN), and dissolved organic sulphur, alongside elevated levels of condensed aromatics, proteins, and unsaturated hydrocarbons, coupled with reduced lignin content in river waters post-wildfire occurrences. Their findings unveiled that DBC constituted 9.5–19.2% of DOC in these water bodies, potentially attributed to atmospheric deposition facilitated by wind dynamics. The Hu *et al.* (2024)[58] review also showed that the thermal effects of wildfire on DOM in watersheds likely impacts the DOM coagulability and reactivity to yield DBPs.

3.1.2 EXO fDOM signal. The results presented in Fig. 2 and 3 also indicated the potential of EXO fDOM sensors as field-deployable instruments to capture the timing and magnitude of climate event impacts on surface waters. The EXO fDOM signal results (without filtration for turbidity removal and with potential for online, real-time applications) showed high correlation (correlation coefficient up to 0.99, Table A4, ESI†) with DOC and UVA_{254}, which have been recorded after filtration for turbidity removal (see Fig. $2a_1$ and b_1 [cyclone] and Fig. $3a_1$ and b_1 [bushfires]).

The fDOM data reported here were obtained from samples collected for laboratory tests, ensuring consistency with other benchmark laboratory-based techniques, rather than from field deployment of the EXO fDOM probe and online data collection. Therefore, further assessments of the probe are necessary to evaluate its potential under online operation under field conditions for extended durations. To address this, we conducted a trial of online data collection from the raw water chamber of a water treatment plant operated by Seqwater in Queensland, drawing water from a reservoir. The trial involved a deployment period over four months (and ongoing), utilising a plastic fouling guard-equipped EXO sonde. Data were collected at ten-minute intervals, immediately following operation of an anti-fouling brush system to clean the probes' windows and tips for each reading. The EXO sonde was powered by four D-size batteries, providing approximately three months of continuous operation under these conditions. However, longer-term power supply options, such as a cable plugged into a power outlet, are available for the sonde in powered sites. Our results demonstrate high performance, reliable, and consistent data collection, even during and after a severe cyclonic event affecting the catchment, reservoir, and plant area. Additionally, the data exhibited strong correlation ($r > 0.95$) with discrete daily A_{254} and monthly DOC data from the plant. The trial revealed the effectiveness of the combined anti-fouling system employed. Calibration checks confirmed the adequacy of monthly checks and indicated the need for approximately bi-monthly recalibration for pH probes, while demonstrating the stability of the fDOM probe over more than four months of operation with less than 5% drift from calibration standards. Detailed quantitative findings from this continuous implementation stage will be provided in a forthcoming publication on the trial.

3.1.3 Chlorophyll-a (Chla). Middle River had the highest post-fire Chla of ~85 μg L^{-1} (21.4 RFU), which was approximately four times greater than the average level of Chla concentrations in subsequent samples. This level of Chla can be associated with a 50% probability of exceeding microcystin health recommended concentrations.[59] The level of ~85 μg L^{-1} of Chla can potentially be an indicator for exceeding the US-EPA recommendation based maximum allowable concentration (MAC) for microcystin in drinking water for children (*i.e.* 23 μg per L Chla potentially indicative of 0.3 μg per L microcystin) and in drinking water (*i.e.* 68 μg per L Chla potentially indicative of 1 μg per L microcystin), and US-EPA recommendation based MAC for microcystin in adult's drinking water (*i.e.* 84 μg per L Chla potentially indicative of 1.6 μg per L microcystin). This highlights the necessity for specific water treatments at DWTPs for Chla and microcystin removals where these occur in source waters. Nonetheless, the maximum recorded Chla for the other sites and samples were <~23 μg L^{-1}, which is below the guideline MAC levels.

The increase in Chla levels following cyclones has been described as relating to the increase in discharges of run-off water (containing nutrients) into surface waters, which can lead to the growth of phytoplankton populations.[32,60] Growth of phytoplankton populations, which consume nutrients, acts as a natural stabilising mechanism and regulates nutrient levels in water sources.[32,61] Peat *et al.* (2005)[62] reported increased Chla levels in catchment stream flows following a bushfire.

3.1.4 Turbidity. Turbidity and Chla demonstrated similar trends (correlations) to each other over time at the sites studied (Fig. 2 and 3). Several studies previously reported an increase in turbidity and sediments in surface waters associated with either burned catchment areas following bushfires[9,25,27,60] or extreme discharge events (*e.g.* following cyclones, typhoons, storms and extreme rainfalls).[29,63–65] Rasul *et al.* (2013)[32] reported increased Chla in a catchment affected by a cyclone.

3.1.5 Nutrients and alkalinity. For Orroral River and Middle River samples collected immediately after bushfires, the TN levels were 1.55 and 5.88 mg L^{-1}, total nitrate and nitrite were 0.207 and 0.055 mg L^{-1} N, TKN was 1.34 and 4.82 mg L^{-1}, TP was 0.18 and 0.31 mg L^{-1}, TOC was 18.2 and 32.6 mg L^{-1} and alkalinity was 144 and 173 mg L^{-1}, respectively. These values are in the range of previously reported studies of catchments impacted by bushfires.[16] The high alkalinity values of samples collected immediately following bushfires may be due to the alkalinity of wood combustion ash.[66]

3.1.6 Heavy metals. Post-bushfire and cyclone concentrations of heavy metals and other elements (*i.e.* Ag, As, B, Ba, Be, Ca, Cd, Co, Cr, Cu, Fe, K, Mg, Mn, Na, Ni, P, Pb, S, Sb, Se, Si, Sr, Ti, V, Zn and U) were all below Australian Drinking Water Guidelines (Table A5, ESI†). Minor effects of fire on streamflow ionic composition have previously been reported.[67,68] This was

explained by (1) the ash element adsorption on the humic and clay complexes in the catchment area prior to discharge into the streams, and (2) the adsorbed elements in the catchment area soil being consumed by the vigorously regrowing vegetation.[67] Johnston and Maher (2022)[24] reported general increases in TSS, DOC, electrical conductivity and several ions (*i.e.* HCO_3^-, SO_4^{2-}, Ca^{2+}, K^+, PO_4^{3-} and NO_3^-) immediately after a severe drought and extensive fires followed by flooding in a large coastal catchment (Macleay River, Australia).

Uzun *et al.* (2020)[69] compared the water quality impacts of two California bushfires (Rocky and Wragg Fires, 2015) to an unburned reference watershed. They reported that the concentrations of DOC, DON, ammonium (NH_4^+/NH_3), and $SUVA_{254}$ levels were significantly higher during the first year (67 ± 40%, 418 ± 125%, 192 ± 120%, and 31 ± 17%, respectively).[69] Similarly, Chen *et al.* (2018)[65] reported major increases in both dissolved nutrients and suspended particulates during storms in the Jurong River Estuary, southeast China. These increases were related to river inflows, surrounding runoff, pore water supply, and nutrients desorbed from scoured sediment.[65]

3.2 fEEM data

Both HIX and BIX data demonstrated potential for capturing the variations in DOM characteristics following the cyclone (Fig. 4). HIX values in the samples collected immediately following the cyclone event were high for both the P03 and P05 sites (0.97 and 0.98, respectively), and slightly decreased in subsequent samples (0.94 and 0.85, respectively). In contrast, BIX was low at these sites immediately after the cyclone event (0.41 and 0.30, respectively), and increased in the subsequent samples (0.53 and 0.48). Heavy rainfall and subsequent surface water flows associated with the cyclone event may increase the terrestrial fraction of humic substances in the DOM pool immediately after the cyclone, resulting in observed increases in HIX and SUVA as well as the observed decreases in BIX.

Xu *et al.* (2016)[70] reported similar increases in HIX and $SUVA_{254}$ after a typhoon in the South Tiaoxi River, China. They reported increases in both HIX (0.75 to 0.79) and DOC (3.17 to 3.64 mg L^{-1}), though a decrease in BIX (0.83 to 0.75), which is consistent with the results of the current study. Similar increases in HIX (0.74 to 0.91) and DOC (2.0 to 5.1 mg L^{-1}) and decreases in BIX (0.81 to 0.79) were reported by Begum *et al.* (2023)[71] following a storm affecting an agricultural watershed in South Korea.

As detailed in Daraei *et al.* (2023),[45] the humic-like components PAR−C_1, PAR-C_2 and PAR-C_4 are among the most common fluorophores found in freshwaters, with a large number of matches in the OpenFluor database library.[72] These are associated with high molecular weight and aromatic terrestrial compounds.[72] PAR-C_3 and PAR-C_5 components are

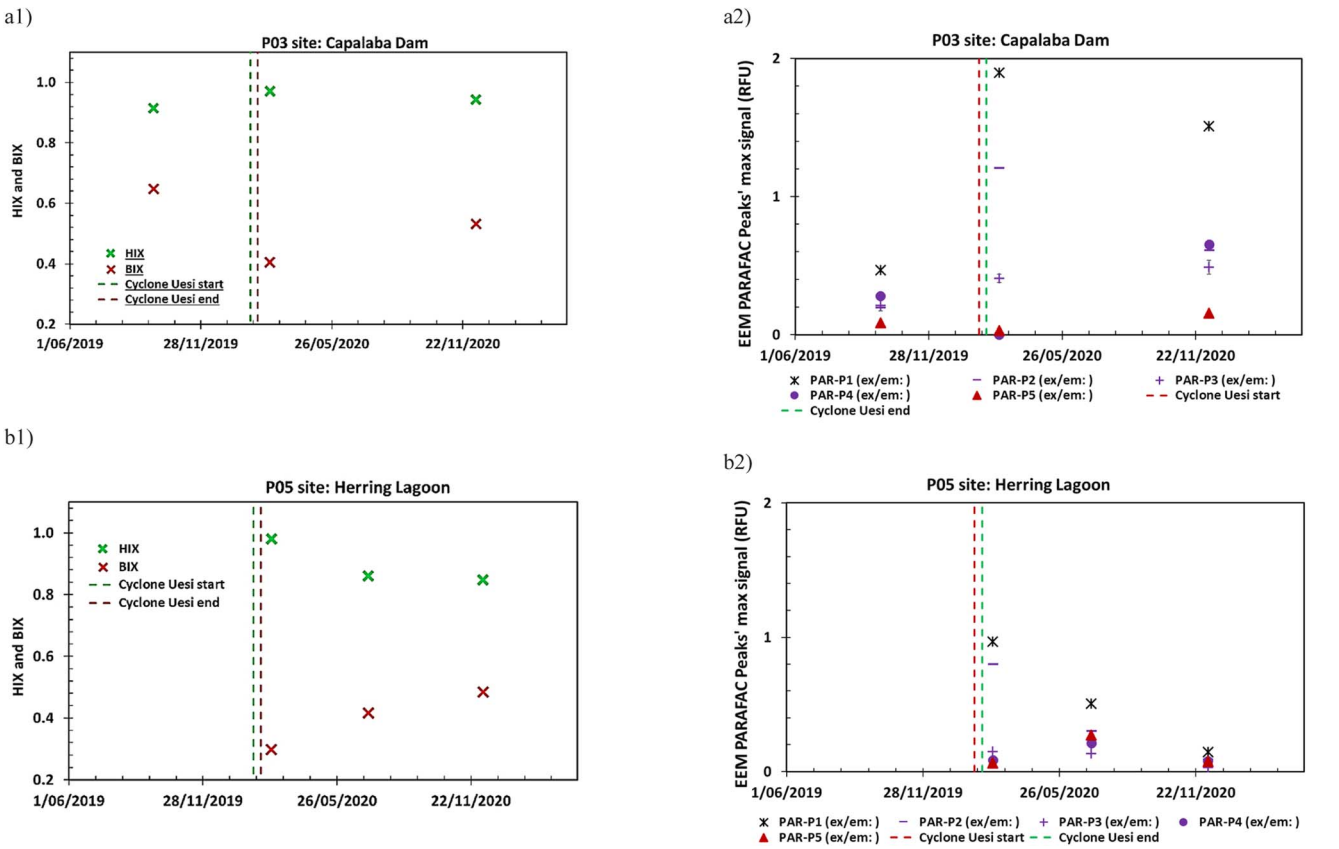

Fig. 4 Chronological variations of (1) FRI based technique indices (HIX and BIX) and (2) PARAFAC based indices (PAR-P1 to PAR-P5) extracted from fEEM data of (a) Leslie Harrison Dam, P03 and (b) Herring Lagoon, P05 surface water sources. *Full-page size graphs are provided in the ESI.†

classified as microbial protein-like components related to the production of DOM within aquatic ecosystems.[43] The PARAFAC results for the P03 and P05 sites were used to provide a new ratio index (sum of protein-like peaks to sum of humic like peaks, *i.e.* ([PAR-C_3 + PAR-C_5]/[PAR-C_1 + PAR-C_2 + PAR-C_4]) which can be similar in nature to the BIX index and likely more reliable due to the robustness of the PARAFAC technique. For sites that experienced the cyclone, the variations of this new ratio index are comparable to BIX index variations. The new index varied from 0.14 (soon after the event) to 0.23 (in the subsequent samples) at site P03 (and from 0.11 to >0.35 at site P05). However, the new index would benefit from further validation, although this is beyond the scope of this study. The PARAFAC components may provide more information on DOM characteristics by being linked with DOM fractions and molecular level characteristic data, though further investigation is required. Nonetheless, the results presented here can provide a basis for future research.

Xu *et al.* (2016)[70] reported a four-component PARAFAC model, including two protein-like components and two humic-like components in samples collected before and after a typhoon-induced heavy rainfall event in the South Tiaoxi River, China. Begum *et al.* (2023)[71] reported a three-component PARAFAC model for DOM in the samples they studied. They reported an increase in the mean protein-like portion of the DOM following the storm, which is not consistent with our results, as well as a decrease in BIX. This could be due to the statistical uncertainty associated with their mean data, as mentioned in their study.

For sites that experienced bushfires, the BIX index demonstrates greater potential than HIX for capturing variation in DOM characteristics (see Fig. 5). In contrast to the sites that experienced the cyclone, high BIX values were found in samples collected immediately after the bushfires, which subsequently decreased over time, with fluctuations likely associated with seasonal effects. This could be due to the discharge of DOM with chromophoric characteristics following bushfires (combustion products and fire extinguishing agents), which differ from those following cyclone events. The Hu *et al.* (2024)[58] review study shows that generally, the proportion of tyrosine-like and humic acid-like FRI showed a decreasing trend after wildfires. The HIX values are generally consistent, with small variations over time. Uzun *et al.* (2020)[69] and Johnston and Maher (2022)[24] reported an opposite HIX trend to what we observed in the current study (*i.e.* increasing soon after the bushfire and then decreasing over time). This might be due to the application of a different formula for the calculation of HIX,[48] which may be another reason for higher reliability of the BIX index for comparisons. However, as a PARAFAC-based alternative index to the BIX, the newly suggested index in our study (*i.e.* [PAR-C_3 + PAR-C_5]/[PAR-C_1 + PAR-C_2 + PAR-C_4]) varied from 0.34 (soon after the event) to <0.20 (in the subsequent samples) at site P01 and from 0.42 to <0.20 at site P11.

3.3 HPSEC data

Weight-averaged apparent molecular weights (WAMWs) were generally higher in the samples collected soon after the cyclone (within approximately two to three weeks, see Fig. 6) than subsequent samples (collected after approximately 10 months, see Fig. 6). This might be due to the presence of a larger amount

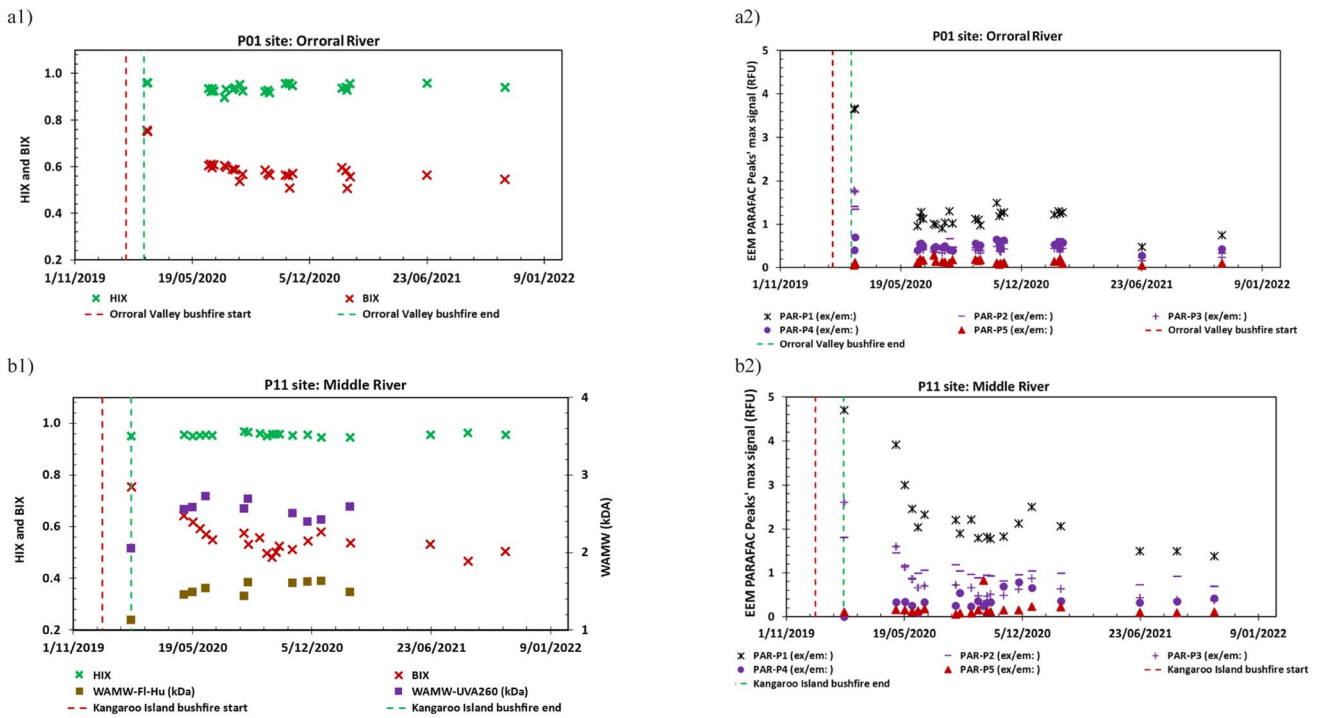

Fig. 5 Chronological variations of the (1) FRI based technique indices (HIX and BIX) and (2) PARAFAC based indices (PAR-P1 to PAR-P5) extracted from fEEM data of (a) Orroral River, P01 and (b) Middle River, P11 surface water sources. *Full-page size graphs are provided in the ESI.†

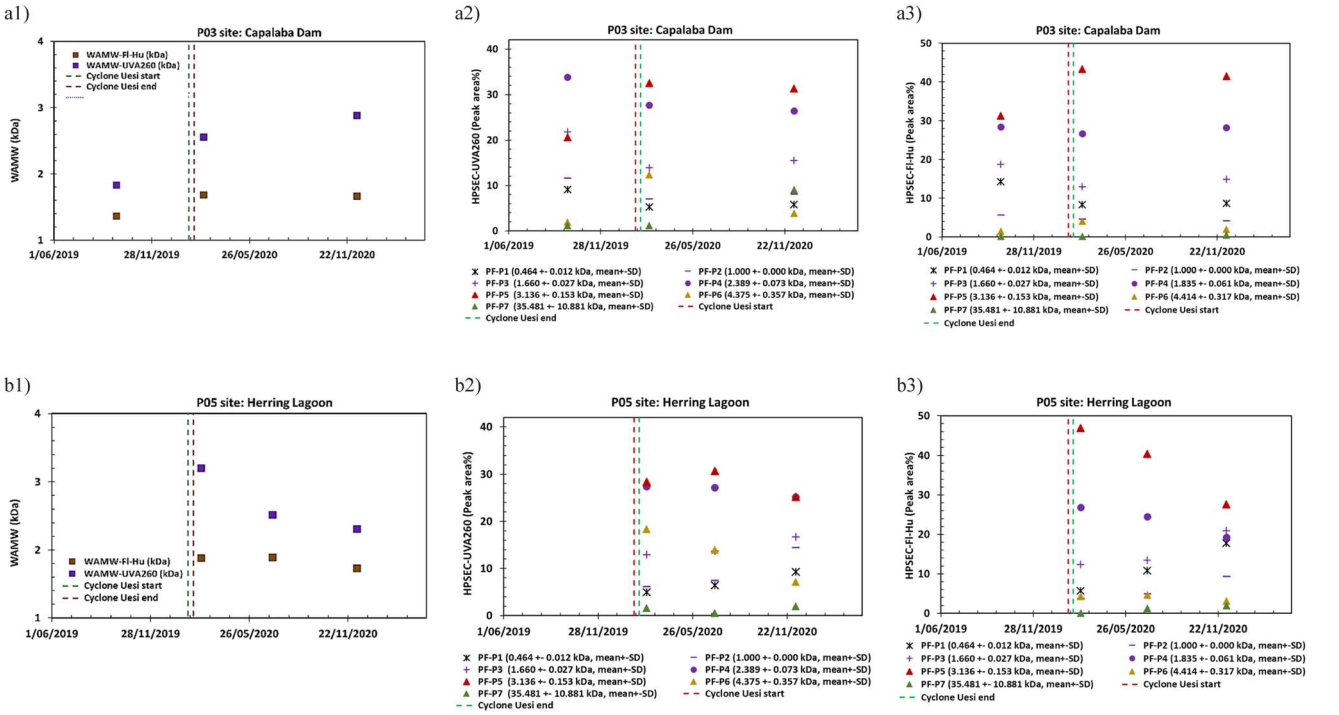

Fig. 6 Chronological variations of the (1) FRI based indices (HIX and BIX), (2) HPSEC-UVA_{260} and (3) HPSEC-Fl-Hu extracted from HPSEC data of (a) Leslie Harrison Dam, P03 and (b) Herring Lagoon, P05 surface water sources. *Full-page size graphs are provided in the ESI.†

of fresh terrestrial DOM with a greater molecular weight discharged into the surface waters during heavy precipitations during the tropical cyclone event.

In contrast, WAMWs were lower soon after bushfires (within approximately two to three weeks, see Fig. 7) than in the subsequent samples (collected after approximately six months). This might be due to the presence of a larger amount of combustion products – including through the airborne smoke and particles,[73] with a lower molecular weight in the samples collected immediately after the bushfire.[74] In Japanese forested

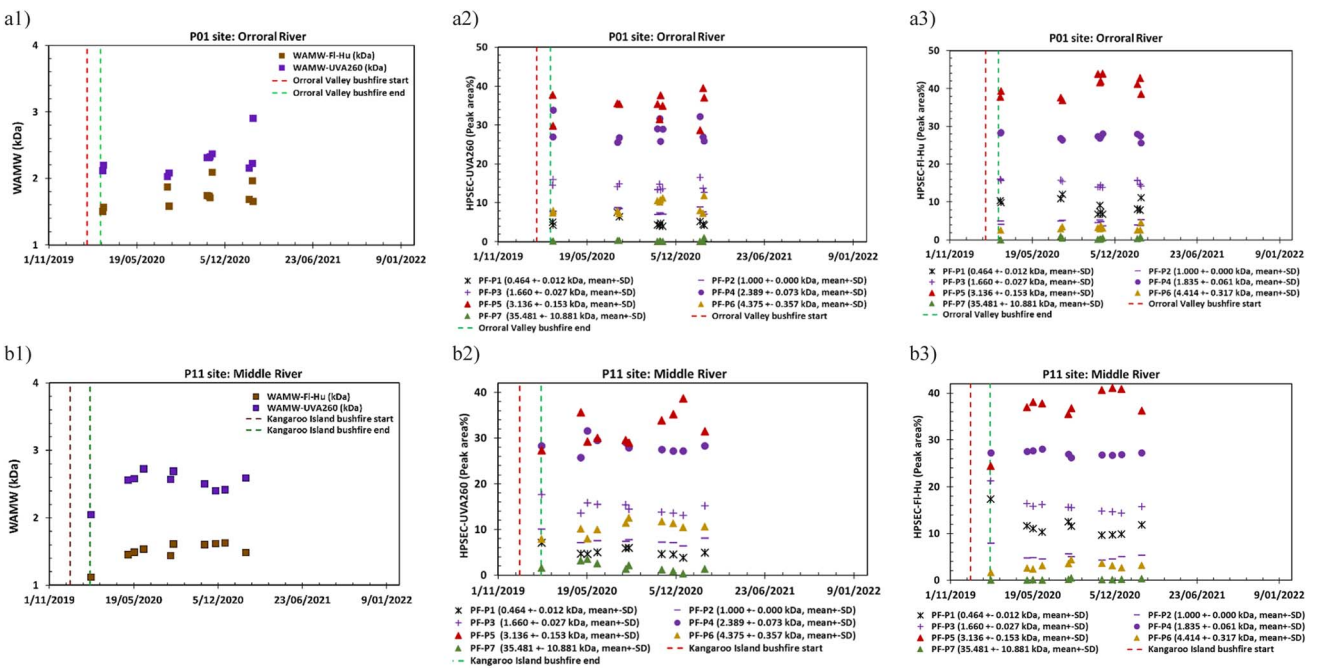

Fig. 7 Chronological variations of the (1) FRI based indices (HIX and BIX), (2) HPSEC-UVA_{260} and (3) HPSEC-Fl-Hu extracted from HPSEC data of (a) Orroral River, P01 and (b) Middle River, P11 surface water sources. *Full-page size graphs are provided in the ESI.†

catchments, Sazawa *et al.* (2018)[75] found that bushfires significantly changed the properties of fulvic acids and increased the concentration of DOC with low molecular weight in surface soil. Similarly, Muri *et al.* (2003)[76] identified the footprint of a historical bushfire (which had occurred in 1948) in northwest Slovenia through the polycyclic aromatic hydrocarbons and black carbon loads, low $SUVA_{254}$ and molecular weight,[77] in discharged sediments.

Seven MW-based components or peaks, called PF-P1 to PF-P7, were identified for the samples studied. The results are presented in Fig. $6a_2$ and b_2 (cyclone) and Fig. $7a_2$ and b_2 (bushfires; for HPSEC-UVA_{260} data) and in Fig. $6a_3$ and b_3 (cyclone) and Fig. $7a_3$ and b_3 (bushfires; for HPSEC-Fl-Hu data) and Table A2, ESI.†

For sites that had experienced the cyclone, concentration of the coloured (chromophoric) dissolved organic matter (CDOM) and fDOM fractions with higher molecular weight (>~3 kDa) indicated a slight decrease after approximately 10 months (Fig. 6). This aligns with WAMW and Sp. colour trends. However, fractions with lower MW (<~3 kDa) increased slightly, which aligns with the BIX trend (Fig. 4). Li *et al.* (2003)[78] reported an increase in WAMW of Nagara River water samples from ~3.0 kDa (a few hours prior to the heavy rainfall starting) to 3.5 kDa (a few days after the heavy rainfall) during a typhoon event in Honsyu, Japan. This aligns with our results (Fig. $6a_1$) whereby WAMW increased from ~1.8 kDa to ~2.6 kDa. Huang *et al.* (2016) reported higher DOC, A_{254}, $SUVA_{254}$, colour, specific colour and WAMW for the DOM pool in urban stormwater, which can occur following cyclones. Moreover, they suggested a likely need for a specific treatment strategy under such conditions.[79] Furthermore, as previously reported,[35,45] up to 73% and 90% of the DOC in P03 and P05 samples, respectively, are removable (coagulable) by an enhanced coagulation process. Also, a high DOC removal rate of 12.6 and 18.5 mg DOC per 100 mg alum were reported for P03 and P05 samples, respectively.[35]

For sites that experienced bushfires, the CDOM and fDOM fractions with higher molecular weight (>~3 kDa) indicated a slight increase with increasing time since fire, which aligns with the WAMW and Sp. colour trends. In contrast, the fractions with lower MW showed a slight decrease with time since fire, which aligns with the BIX trend. This general increase in the humic substance indices could be due to increased discharge of soil leachate biomass into streams. This can happen under particular conditions of rapid revegetation of burned catchment areas following bushfires[27] and using minerals available in the ash trapped in the soil of the burned catchment area,[24,67] increased catchment water yield[24] and soil erosion.[80] This can increase colour, humic index, and WAMW in corresponding streams and water sources.

Similar observations have been previously reported in several studies. Begum *et al.* (2022)[81] studied four DOM sources (*i.e.* field soil, litter, reed and manure), while Begum *et al.* (2023)[71] studied five further DOM sources (*i.e.* soil, leaves, compost, a sewage plant effluent and manure). In both studies, they reported that the highest HIX level was from soil-sourced DOM. Shams (2018)[82] conducted a comprehensive two year study on DOM concentration and characteristics and their relationships to trihalomethane formation potential (THMFP) and haloacetic acid formation potential (HAAFP) following a severe bushfire on the eastern slopes of the Rocky Mountains in southwestern Alberta, Canada. Shams (2018)[82] reported increases in DOC concentration (from <2 mg L^{-1} to >6 mg L^{-1}), DOM hydrophobicity and disinfection by-product formation potential (DBPFP) following bushfires (and even more following salvage-logging following the fire) and during high discharge events in headwater streams. Shams (2018)[82] suggested challenges associated with DOM treatability and several detrimental consequences (*e.g.* carbonaceous DBPFP, coagulant demand and membrane fouling) for DWTP intake waters severely impacted by bushfires. In our study, only 62% and 52% of the DOC concentrations in samples collected from sites P01 and P11, respectively, soon after the bushfire events could be removed through coagulation processes, suggesting lower coagulability than DOC content in sites impacted by the cyclone.[35,45] Furthermore, a lower DOC removal rate of 9.0 and 8.4 mg DOC per 100 mg alum were observed, as reported in Daraei *et al.* (2023).

Our study was conceived after the extreme events of the 2019/2020 bushfires and the 2020 Tropical Cyclone Uesi had occurred, initially in the context of acquiring representative samples of surface waters following such events for a better understanding of changes in the concentrations and characteristics of DOM. This will contribute towards an improved understanding of the impacts of such extreme climate events on the ecological health of fresh surface waters and water resources used for drinking and other purposes. Subsequently, improved predictive capability for the treatment of surface waters following such extreme events for securing drinking water supply was investigated, as reported by Daraei *et al.* (2021).[83] Hohner *et al.* (2017)[84] concluded that the greatest treatment challenges were likely to be immediately after a bushfire and subsequent flow events. However, they suggested a longer-term investigation of the duration of the possible post-fire effects on water treatment process efficiency.

4 Conclusion

This study monitored water quality parameters following bushfires and a cyclone by applying both routine and advanced analytical techniques. The study generated novel insights into potential impacts of these events on surface water quality and the timeframe and processes of subsequent water quality stabilisation. Observed high DOM concentrations (measured as DOC and A_{254}) soon after the extreme events (up to >30 mg L^{-1}) can influence the treatment process efficiency and costs at DWTPs. High DOM concentrations, colour and turbidity can also influence aquatic ecological health. A useful feature of this study was chronological tracking of DOC concentration over a relatively long period of 1–2 years, which revealed a general decreasing trend of DOC concentration, likely due to dilution following precipitation events. However, the DOM present in the surface water associated with the cyclone event had different characteristics ($SUVA_{254}$, BIX, WAMW, DOC

coagulability and removal rate) than the DOM present in the surface water associated with bushfire events. The mostly aligned trends exhibited by EXO $fDOM_s$ with DOC and A_{254} indicate the potential benefit of using fDOM field-deployable sensors for continuous/real-time DOM monitoring and water quality determination for freshwater at sites that have experienced extreme climate events.

Conflicts of interest

The authors declared that they had no conflicts of interest with respect to their authorship or the publication of this article.

Acknowledgements

This research was funded by the Australian Government through the Australian Research Council (ARC LP160100217). The authors would like to express their gratitude to all project partners (*i.e.* Xylem Analytics Australia, Seqwater, and Melbourne Water) for their contributions.

References

1 A. I. Filkov, T. Ngo, S. Matthews, S. Telfer and T. D. Penman, Impact of Australia's catastrophic 2019/20 bushfire season on communities and environment. Retrospective analysis and current trends, *J. Saf. Sci. Resil.*, 2020, **1**, 44–56.

2 L. M. Mosley, D. S. Sharp and S. Singh, Effects of a tropical cyclone on the drinking-water quality of a remote Pacific island, *Disasters*, 2004, **28**, 405–417.

3 H. W. Paerl, N. S. Hall, A. G. Hounshell, R. A. Luettich Jr, K. L. Rossignol, C. L. Osburn and J. Bales, Recent increase in catastrophic tropical cyclone flooding in coastal North Carolina, USA: Long-term observations suggest a regime shift, *Sci. Rep.*, 2019, **9**, 1–9.

4 S. J. Khan, D. Deere, F. D. Leusch, A. Humpage, M. Jenkins and D. Cunliffe, Extreme weather events: Should drinking water quality management systems adapt to changing risk profiles?, *Water Res.*, 2015, **85**, 124–136.

5 R. Mannik, A. Herron, P. Hill, R. Brown and R. Moran, Estimating the Change in Streamflow Resulting from the 2003 and 2006/2007 Bushf Res in Southeastern Australia, *Australas. J. Water Resour.*, 2013, **16**, 107–120.

6 R. H. Nolan, D. M. Bowman, H. Clarke, K. Haynes, M. K. Ooi, O. F. Price, G. J. Williamson, J. Whittaker, M. Bedward and M. M. Boer, What do the Australian Black Summer fires signify for the global fire crisis?, *Fire*, 2021, **4**, 1–18.

7 G. J. Van Oldenborgh, F. Krikken, S. Lewis, N. J. Leach, F. Lehner, K. R. Saunders, M. Van Weele, K. Haustein, S. Li and D. Wallom, Attribution of the Australian bushfire risk to anthropogenic climate change, *Nat. Hazards Earth Syst. Sci.*, 2021, **21**, 941–960.

8 E. S. Quill, M. J. Angove, D. W. Morton and B. B. Johnson, Characterisation of dissolved organic matter in water extracts of thermally altered plant species found in box-ironbark forests, *Aust. J. Soil Res.*, 2010, **48**, 693–704.

9 T. K. Biswas, F. Karim, A. Kumar, S. Wilkinson, J. Guerschman, G. Rees, P. McInerney, B. Zampatti, A. Sullivan, P. Nyman, G. J. Sheridan and K. Joehnk, 2019-2020 Bushfire impacts on sediment and contaminant transport following rainfall in the Upper Murray River catchment, *Integrated Environ. Assess. Manag.*, 2021, **17**, 1203–1214.

10 J. Neris, C. Santin, R. Lew, P. R. Robichaud, W. J. Elliot, S. A. Lewis, G. Sheridan, A. M. Rohlfs, Q. Ollivier, L. Oliveira and S. H. Doerr, Designing tools to predict and mitigate impacts on water quality following the Australian 2019/2020 wildfires: Insights from Sydney's largest water supply catchment, *Integrated Environ. Assess. Manag.*, 2021, **17**, 1151–1161.

11 J. Heisler, P. Glibert, J. Burkholder, D. Anderson, W. Cochlan, W. Dennison, C. Gobler, Q. Dortch, C. Heil, E. Humphries, A. Lewitus, R. Magnien, H. Marshall, K. Sellner, D. Stockwell, D. Stoecker and M. Suddleson, Eutrophication and Harmful Algal Blooms: A Scientific Consensus, *Harmful Algae*, 2008, **8**, 3–13.

12 A. Teksoy, U. Alkan and H. S. Baskaya, Influence of the treatment process combinations on the formation of THM species in water, *Sep. Purif. Technol.*, 2008, **61**, 447–454.

13 D. M. Golea, A. Upton, P. Jarvis, G. Moore, S. Sutherland, S. A. Parsons and S. J. Judd, THM and HAA formation from NOM in raw and treated surface waters, *Water Res.*, 2017, **112**, 226–235.

14 B. Wright, B. D. Stanford, A. Reinert, J. C. Routt, S. J. Khan and J. F. Debroux, Managing water quality impacts from drought on drinking water supplies, *J. Water Supply Res. Technol.*, 2014, **63**, 179–188.

15 H. Smith, J. Cawson, G. Sheridan and P. Lane, *Desktop Review–Impact of Bushfires on Water Quality*, University of Melbourne, 2011.

16 K. Joehnk, T. Biswas, F. Karim, A. Kumar, J. Guerschman, S. Wilkinson, G. Rees, P. McInerney, B. Zampatti and A. Sullivan, *Water Quality Responses for Post 2019-20 Bushfires Floods in South Eastern Australia: a Catchment Scale Analysis: A Technical Report for the CSIRO Strategic Bushfire Project 2020*, Australia's National Science Agency, Canberra, Australia, 2020.

17 P. Niquette, P. Servais and R. Savoir, Bacterial dynamics in the drinking water distribution system of Brussels, *Water Res.*, 2001, **35**, 675–682.

18 D. P. Kreutzweiser and S. S. Capell, Benthic microbial utilization of differential dissolved organic matter sources in a forest headwater stream, *Can. J. For. Res.*, 2003, **33**, 1444–1451.

19 K. C. Young, K. M. Docherty, P. A. Maurice and S. D. Bridgham, Degradation of surface-water dissolved organic matter: influences of DOM chemical characteristics and microbial populations, *Hydrobiologia*, 2005, **539**, 1–11.

20 K. Kaiser and W. Zech, Competitive Sorption of Dissolved Organic Matter Fractions to Soils and Related Mineral Phases, *Soil Sci. Soc. Am. J.*, 1997, **61**, 64–69.

21 *Photobiogeochemistry of Organic Matter: Principles and Practices in Water Environments*, ed. K. M. Mostofa, T. Yoshioka, A. Mottaleb and D. Vione, Springer Science & Business Media, Berlin Heidelberg, 2012.
22 L. M. Mosley, T. Wallace, J. Rahman, T. Roberts and M. Gibbs, An integrated model to predict and prevent hypoxia in floodplain-river systems, *J. Environ. Manage.*, 2021, **286**, 1–13.
23 DAWE, Blackwater events and water quality, **https://www.waterquality.gov.au/issues/blackwater-events**, accessed 20/08/2022.
24 S. G. Johnston and D. T. Maher, Drought, megafires and flood-climate extreme impacts on catchment-scale river water quality on Australia's east coast, *Water Res.*, 2022, **218**, 1–13.
25 L. R. Sherson, D. J. Van Horn, J. D. Gomez-Velez, L. J. Crossey and C. N. Dahm, Nutrient dynamics in an alpine headwater stream: use of continuous water quality sensors to examine responses to wildfire and precipitation events, *Hydrol. Process.*, 2015, **29**, 3193–3207.
26 M. Basso, M. Mateus, T. B. Ramos and D. C. Vieira, Potential post-fire impacts on a water supply reservoir: an integrated watershed-reservoir approach, *Front. Environ. Sci.*, 2021, **9**, 1–13.
27 I. White, A. Wade, M. Worthy, N. Mueller, T. Daniell and R. Wasson, The vulnerability of water supply catchments to bushfires: impacts of the January 2003 wildfires on the Australian Capital Territory, *Australas. J. Water Resour.*, 2006, **10**, 179–194.
28 S. S. Kaushal, A. J. Gold, S. Bernal and J. L. Tank, Diverse water quality responses to extreme climate events: an introduction, *Biogeochemistry*, 2018, **141**, 273–279.
29 A. M. Hurst, M. J. Edwards, M. Chipps, B. Jefferson and S. A. Parsons, The impact of rainstorm events on coagulation and clarifier performance in potable water treatment, *Sci. Total Environ.*, 2004, **321**, 219–230.
30 S. Hoffmeister, K. Murphy, C. Cascone, J. L. Ledesma and S. Köhler, Evaluating the accuracy of two in situ optical sensors to estimate DOC concentrations for drinking water production, *Environ. Sci.: Water Res. Technol.*, 2020, **6**, 2891–2901.
31 G. de Oliveira, E. Bertone, R. Stewart, J. Awad, A. Holland, K. O'Halloran and S. Bird, Multi-Parameter Compensation Method for Accurate In Situ Fluorescent Dissolved Organic Matter Monitoring and Properties Characterization, *Water*, 2018, **10**, 1146.
32 E. Rasul, T. Inoue, S. Aoki, K. Yokota, Y. Matsumoto and Y. Okubo, Influence of tropical cyclone on the water quality of Atsumi Bay, *J. Water Environ. Technol.*, 2013, **11**, 439–451.
33 X. F. Gao, H. H. Chen, B. H. Gu, E. Jeppesen, Y. Y. Xue and J. Yang, Particulate organic matter as causative factor to eutrophication of subtropical deep freshwater: Role of typhoon (tropical cyclone) in the nutrient cycling, *Water Res.*, 2021, **188**, 1–10.
34 H. Daraei, E. Bertone, J. Awad, R. A. Stewart, C. W. Chow, J. Duan, A. Mussared and J. Van Leeuwen, A novel mathematical template for developing fDOM probe fluorescence signal correction models in freshwaters, *J. Environ. Sci.*, 2023, 1–15.
35 H. Daraei, J. Awad, E. Bertone, R. A. Stewart, C. W. K. Chow, J. M. Duan, J. Creamer and J. Van Leeuwen, DOC signal-based alum dose control for drinking water treatment plants, *J. Water Process Eng.*, 2023, **54**, 103934.
36 *BOM_report, Tropical Cyclone Uesi 4 – 14 February 2020*, **http://www.bom.gov.au/cyclone/history/Uesi.shtml**, accessed 11/11/2020.
37 N. Benger and B. Chapman, Seasonal climate summary for the southern hemisphere (summer 2019–20): a summer of extremes, *J. South. Hemisph. Earth Syst. Sci.*, 2023, **73**(2), 83–101.
38 L. Richards, N. Brew and L. Smith, Parliament of Australia; 2019–20 Australian bushfires-frequently asked questions: a quick guide., **https://www.aph.gov.au/About_Parliament/Parliamentary_Departments/Parliamentary_Library/pubs/rp/rp1920/Quick_Guides/AustralianBushfires**, accessed 11/12/2020.
39 J. Liu, D. Freudenberger and S. Lim, Mapping burned areas and land-uses in Kangaroo Island using an object-based image classification framework and Landsat 8 Imagery from Google Earth Engine, *Geomatics, Nat. Hazards Risk*, 2022, **13**, 1867–1897.
40 Australian_government_report, *Australian Capital Territory, January – February 2020 Bushfires - Black Summer*, **https://knowledge.aidr.org.au/resources/black-summer-bushfires-act-2020/#:~:text=Thefireeventuallyburned82%2C700,intheACT'shistory**, accessed 07/10/2023.
41 Australian_government_report, A near-stationary coastal trough over south-east Queensland from 6 February 2020 generated persistent showers and thunderstorms until the middle of the month, with locally heavy falls in some areas, **https://knowledge.aidr.org.au/resources/heavy-rainfall-and-floods-queensland-february-2020/#:~:text=BetweenFridaynighton7,QueenslandandtheDarlingDowns**, accessed 01/09/2023.
42 User_manual, YSI Incorporated, a Xylem brand, *EXO User Manual*, **https://www.ysi.com/filelibrary/documents/manuals/exo-user-manual-web.pdf**, accessed 18/5/2021.
43 H. Daraei, P. D. Intwala, E. Bertone, J. Awad, R. A. Stewart, C. W. Chow, J. Duan and J. van Leeuwen, Enhanced electrocoagulation process for natural organic matter removal from surface drinking water sources: coagulant dose control & organic matter characteristics, *Environ. Sci.: Water Res. Technol.*, 2023, **9**, 62–73.
44 *Standard Methods for the Examination of Water and Wastewater*, ed. R. B. Baird, A. D. Eaton and E. W. Rice, American Public Health Association, American Water Works Association, Water Environment Federation, Washington, DC, 2017.
45 H. Daraei, E. Bertone, J. Awad, R. A. Stewart, C. W. Chow, J. Duan and J. Van Leeuwen, A multi-analytical approach to investigate DOM dynamics and alum dose control in enhanced coagulation process using wide-ranging surface waters, *J. Water Process Eng.*, 2023, **56**, 104368.

46 K. R. Murphy, C. A. Stedmon, D. Graeber and R. Bro, Fluorescence spectroscopy and multi-way techniques. PARAFAC, *Anal. Methods*, 2013, **5**, 6557–6566.
47 A. Huguet, L. Vacher, S. Relexans, S. Saubusse, J. M. Froidefond and E. Parlanti, Properties of fluorescent dissolved organic matter in the Gironde Estuary, *Org. Geochem.*, 2009, **40**, 706–719.
48 T. Ohno, Fluorescence inner-filtering correction for determining the humification index of dissolved organic matter, *Environ. Sci. Technol.*, 2002, **36**, 742–746.
49 C. A. Stedmon, S. Markager and R. Bro, Tracing dissolved organic matter in aquatic environments using a new approach to fluorescence spectroscopy, *Mar. Chem.*, 2003, **82**, 239–254.
50 C. W. Chow, R. Fabris, J. Van Leeuwen, D. Wang and M. Drikast, Assessing natural organic matter treatability using high performance size exclusion chromatography, *Environ. Sci. Technol.*, 2008, **42**, 6683–6689.
51 M. Karakaplan, Fitting Lorentzian peaks with evolutionary genetic algorithm based on stochastic search procedure, *Anal. Chim. Acta*, 2007, **587**, 235–239.
52 M. Sirotiak, L. Blinova and A. Bartosova, Effect of selected extinguishing agents on organic carbon and nutrients leaching from burned soil, *J. Civ. Eng. Construct. Technol.*, 2017, **6**, 45–54.
53 H. Chen, H. Uzun, A. T. Chow and T. Karanfil, Low water treatability efficiency of wildfire-induced dissolved organic matter and disinfection by-product precursors, *Water Res.*, 2020, **184**, 116111.
54 C. N. Spencer, K. O. Gabel and F. R. Hauer, Wildfire effects on stream food webs and nutrient dynamics in Glacier National Park, USA, *For. Ecol. Manag.*, 2003, **178**, 141–153.
55 E. D. Stein, J. S. Brown, T. S. Hogue, M. P. Burke and A. Kinoshita, Stormwater contaminant loading following southern California wildfires, *Environ. Toxicol. Chem.*, 2012, **31**, 2625–2638.
56 W. Tang, J. Llort, J. Weis, M. M. Perron, S. Basart, Z. Li, S. Sathyendranath, T. Jackson, E. Sanz Rodriguez and B. C. Proemse, Widespread phytoplankton blooms triggered by 2019–2020 Australian wildfires, *Nature*, 2021, **597**, 370–375.
57 Y. Xu, X. Wang, Q. Ou, Z. Zhou, J. P. van der Hoek and G. Liu, Appearance of Recalcitrant Dissolved Black Carbon and Dissolved Organic Sulfur in River Waters Following Wildfire Events, *Environ. Sci. Technol.*, 2024, **58**(16), 7165–7175.
58 J. Hu, R. Xiao, R. Zhang, Z. Wu, F. Jiang, C. Ye, R. Qu and W. Chu, Application of EEM fluorescence spectroscopy for characterizing organic DBP precursors in different water sources: a review, *AQUA—Water Infrastructure, Ecosystems and Society*, 2024, **73**, 464–486.
59 J. W. Hollister and B. J. Kreakie, Associations between chlorophyll a and various microcystin health advisory concentrations, *F1000Research*, 2016, **5**, 1–24.
60 A. L. Khan, E. R. Sokol, D. M. McKnight, J. F. Saunders, A. K. Hohner and R. S. Summers, Phytoplankton drivers of dissolved organic material production in Colorado reservoirs and the formation of disinfection by-products, *Front. Environ. Sci.*, 2021, **9**, 1–13.
61 M. Okbah, Nitrogen and phosphorus species of Lake Burullus water (Egypt), *Egypt. J. Aquat. Res.*, 2005, **31**, 186–198.
62 M. Peat, H. Chester and R. Norris, River ecosystem response to bushfire disturbance: interaction with flow regulation, *Aust. For.*, 2005, **68**, 153–161.
63 D. K. Ralston, B. Yellen, J. D. Woodruff and S. Fernald, Turbidity hysteresis in an estuary and tidal river following an extreme discharge event, *Geophys. Res. Lett.*, 2020, **47**, 1–10.
64 C.-S. Lee, Y.-C. Lee and H.-M. Chiang, Abrupt state change of river water quality (turbidity): Effect of extreme rainfalls and typhoons, *Sci. Total Environ.*, 2016, **557**, 91–101.
65 N. Chen, M. D. Krom, Y. Wu, D. Yu and H. Hong, Storm induced estuarine turbidity maxima and controls on nutrient fluxes across river-estuary-coast continuum, *Sci. Total Environ.*, 2018, **628**, 1108–1120.
66 R. Ferraz de Almeida, J. E. Rodrigues Mikhael, F. Oliveira Franco, L. M. Fonseca Santana and B. Wendling, Measuring the labile and recalcitrant pools of carbon and nitrogen in forested and agricultural soils: A study under tropical conditions, *Forests*, 2019, **10**, 1–11.
67 E. Davis, Prescribed fire in Arizona chaparral: effects on stream water quality, *For. Ecol. Manag.*, 1989, **26**, 189–206.
68 C. Johnson and P. Needham, Ionic composition of Sagehen Creek, California, following an adjacent fire, *Ecology*, 1966, **47**, 636–639.
69 H. Uzun, R. A. Dahlgren, C. Olivares, C. U. Erdem, T. Karanfil and A. T. Chow, Two years of post-wildfire impacts on dissolved organic matter, nitrogen, and precursors of disinfection by-products in California stream waters, *Water Res.*, 2020, **181**, 1–12.
70 B. Xu, J. Li, Q. Huang, Q. Gong and L. Li, Impacts of land use patterns and typhoon-induced heavy rainfall event on dissolved organic matter properties in the South Tiaoxi River, China, *Environ. Earth Sci.*, 2016, **75**, 1–15.
71 M. S. Begum, H.-Y. Park, H.-S. Shin, B.-J. Lee and J. Hur, Separately tracking the sources of hydrophobic and hydrophilic dissolved organic matter during a storm event in an agricultural watershed, *Sci. Total Environ.*, 2023, 1–10.
72 K. R. Murphy, C. A. Stedmon, P. Wenig and R. Bro, OpenFluor- an online spectral library of auto-fluorescence by organic compounds in the environment, *Anal. Methods*, 2014, **6**, 658–661.
73 S. Vardoulakis, G. Marks and M. J. Abramson, Lessons learned from the Australian bushfires: climate change, air pollution, and public health, *JAMA Intern. Med.*, 2020, **180**, 635–636.
74 A. L. Sullivan and R. Ball, Thermal decomposition and combustion chemistry of cellulosic biomass, *Atmos. Environ.*, 2012, **47**, 133–141.
75 K. Sazawa, H. Yoshida, K. Okusu, N. Hata and H. Kuramitz, Effects of forest fire on the properties of soil and humic substances extracted from forest soil in Gunma, Japan, *Environ. Sci. Pollut. Res.*, 2018, **25**, 30325–30338.

76 G. Muri, S. G. Wakeham and J. Faganeli, Polycyclic aromatic hydrocarbons and black carbon in sediments of a remote alpine lake (Lake Planina, northwest Slovenia), *Environmental Toxicology and Chemistry: An International Journal*, 2003, **22**, 1009–1016.
77 J.-J. Wang, R. A. Dahlgren, M. S. Ersan, T. Karanfil and A. T. Chow, Wildfire altering terrestrial precursors of disinfection byproducts in forest detritus, *Environ. Sci. Technol.*, 2015, **49**, 5921–5929.
78 F. Li, A. Yuasa, H. Chiharada and Y. Matsui, Storm impacts upon the composition of organic matrices in Nagara River—A study based on molecular weight and activated carbon adsorbability, *Water Res.*, 2003, **37**, 4027–4037.
79 H. Huang, C. W. Chow and B. Jin, Characterisation of dissolved organic matter in stormwater using high-performance size exclusion chromatography, *J. Environ. Sci.*, 2016, **42**, 236–245.
80 P. K. Rustomji and P. B. Hairsine, *Revegetation of Water Supply Catchments Following Bushfire: A Review of the Scientific Literature Relevant to the Lower Cotter Catchment*, CSIRO Land and Water, 2006.
81 M. S. Begum, M.-H. Lee, T. J. Park, S. Y. Lee, K.-H. Shin, H.-S. Shin, M. Chen and J. Hur, Source tracking of dissolved organic nitrogen at the molecular level during storm events in an agricultural watershed, *Sci. Total Environ.*, 2022, **810**, 1–11.
82 S. Shams, PhD, University of Waterloo, 2018.
83 H. Daraei, J. Awad, E. Bertone, R. A. Stewart, C. W. K. Chow, J. Duan and J. van Leeuwen, *Presented in Part at the 24th International Congress on Modelling and Simulation (Modsim2021)*, Brisbane, Queensland, Australia, 2021.
84 A. K. Hohner, L. G. Terry, E. B. Townsend, R. S. Summers and F. L. Rosario-Ortiz, Water treatment process evaluation of wildfire-affected sediment leachates, *Environ. Sci.: Water Res. Technol.*, 2017, **3**, 352–365.